BIOMOLECULES & THERAPEUTICS

Original Article
Biomol Ther 26(3), 282-289 (2018)

Designing Tyrosinase siRNAs by Multiple Prediction Algorithms and Evaluation of Their Anti-Melanogenic Effects

Ok-Seon Kwon[1,†], Soo-Jung Kwon[1,†], Jin Sang Kim[2], Gunbong Lee[2], Han-Joo Maeng[3], Jeongmi Lee[4], Gwi Seo Hwang[5], Hyuk-Jin Cha[1,*] and Kwang-Hoon Chun[3,*]

[1]*Department of Life Sciences, Sogang University, Seoul 04107,*
[2]*Leaders Cosmetics Co., Ltd., Anseong 17599,*
[3]*Gachon Institute of Pharmaceutical Sciences, College of Pharmacy, Gachon University, Incheon 21936,*
[4]*School of Pharmacy, Sungkyunkwan University, Suwon 16419,*
[5]*Laboratory of Cell Differentiation Research, College of Korean Medicine, Gachon University, Seongnam 13120, Republic of Korea*

Abstract

Melanin is a pigment produced from tyrosine in melanocytes. Although melanin has a protective role against UVB radiation-induced damage, it is also associated with the development of melanoma and darker skin tone. Tyrosinase is a key enzyme in melanin synthesis, which regulates the rate-limiting step during conversion of tyrosine into DOPA and dopaquinone. To develop effective RNA interference therapeutics, we designed a melanin siRNA pool by applying multiple prediction programs to reduce human tyrosinase levels. First, 272 siRNAs passed the target accessibility evaluation using the *RNAxs* program. Then we selected 34 siRNA sequences with ΔG ≥-34.6 kcal/mol, *i-Score* value ≥65, and *siRNA scales score* ≤30. siRNAs were designed as 19-bp RNA duplexes with an asymmetric 3' overhang at the 3' end of the antisense strand. We tested if these siRNAs effectively reduced tyrosinase gene expression using qRT-PCR and found that 17 siRNA sequences were more effective than commercially available siRNA. Three siRNAs further tested showed an effective visual color change in MNT-1 human cells without cytotoxic effects, indicating these sequences are anti-melanogenic. Our study revealed that human tyrosinase siRNAs could be efficiently designed using multiple prediction algorithms.

Key Words: Tyrosinase, Melanin, siRNA, Melanocytes, Whitening

INTRODUCTION

Human skin color is determined mainly by the pigment melanin, which is produced by melanocytes in the epidermis. Melanin production is induced upon skin exposure to ultraviolet radiation, and it is transported to keratinocytes in a vesicle-mediated manner (Slominski *et al*., 2004). Two types of melanin, eumelanin and pheomelanin, are produced from L-tyrosine through a multi-step process. Eumelanin is a dark, brown-black insoluble polymer responsible for dark skin color (Slominski *et al*., 2004). The rate-limiting step in melanogenesis is the conversion of L-tyrosine into L-dihydroxyphenylalanine (L-DOPA) by tyrosinase (Lerner and Fitzpatrick, 1950; Hearing and Tsukamoto, 1991). For cosmetic and pharmaceutical purposes, many tyrosinase-inhibiting agents have been developed to manage skin pigmentation, such as hydroquinone (1,4-dihydroxybenzene), arbutin, azelaic acid (1,7-heptanedicarboxyilic acid), and others (Gillbro and Olsson, 2011). Even though their anti-pigmentation effects have been well-established, the risk of side effects has brought about hesitation for continuous use of tyrosinase inhibitors, as shown by the fact that hydroquinone formulations with concentrations over 1% have been banned in Europe (Gillbro and Olsson, 2011).

RNA interference (RNAi) was first discovered as an antiviral defense mechanism in the nematode *Caenorhabditis elegans* in which double-stranded RNAs (dsRNAs) trigger gene silencing of complementary mRNA sequences (Fire *et al*., 1998). Thereafter, artificially synthesized short interfering RNAs (siRNAs) were observed to be processed in mammalian cells (Elbashir *et al*., 2001a). RNAi processing consists of several

Open Access **https://doi.org/10.4062/biomolther.2017.115**

Received May 30, 2017 **Revised** Aug 3, 2017 **Accepted** Aug 7, 2017
Published Online Dec 8, 2017

***Corresponding Authors**
E-mail: khchun@gachon.ac.kr (Chun KH), hjcha@sogang.ac.kr (Cha HJ)
Tel: +82-32-820-4951 (Chun KH), +82-2-705-4761 (Cha HJ)
Fax: +82-32-820-4823 (Chun KH), +82-2-704-3601 (Cha HJ)
[†]The first two authors contributed equally to this work.

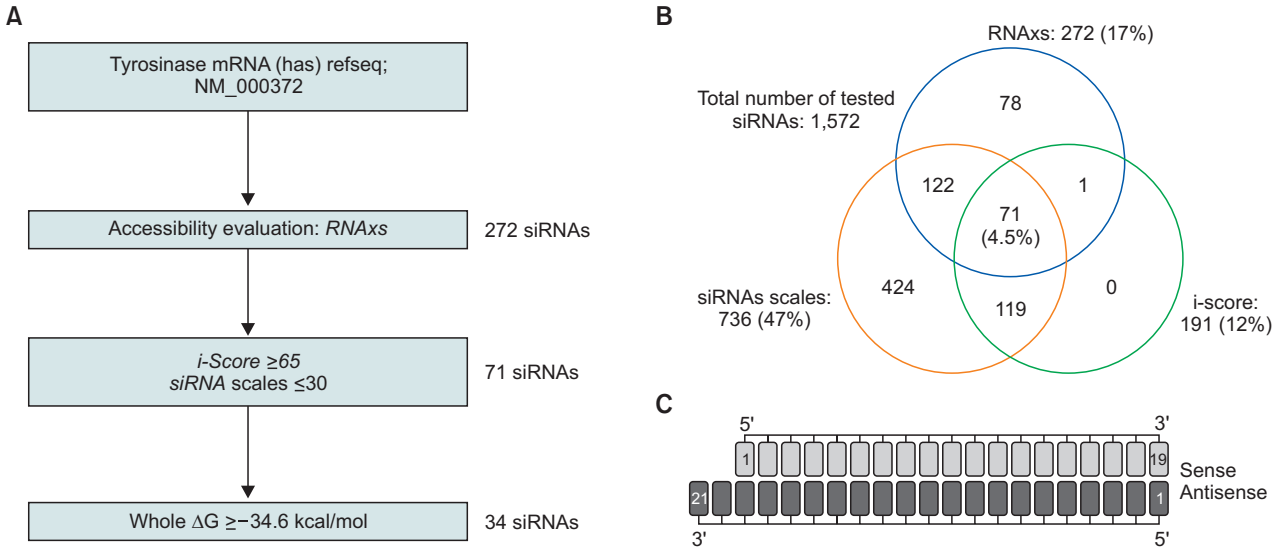

Fig. 1. Experimental scheme for selecting the best tyrosinase-targeted siRNAs. (A) Tyrosinase mRNA sequence was obtained from NCBI nucleotide dataset (Refseq id NM_000372). siRNAs were filtered from *RNAxs* using default parameters and then further selected according to the scores acquired from *i-Score* ≥65 and *siRNA scales* ≤30 prediction softwares, with whole ΔG values ≥-34.6 kcal/mol. (B) Distribution diagram of selected siRNAs according to the algorithms used. Numbers indicate siRNA identity. Percentages represent the population of siRNA from total number of tested siRNAs. (C) The structure of siRNA. Sense strands have 19 nt while antisense strands have 19+2 nt skeletons. 3' end overhangs were designed only for the antisense strand.

steps; siRNA generation by dsRNA cleavage by Dicer, assembly of siRNA with the RNA-induced silencing complex (RISC), separation of siRNA strands (the sense (passenger) and antisense (guide) strands), binding of the antisense strand to mRNA with a complementary sequence, and degradation of mRNA by Argonaute 2 (Ago2) (Engels, 2013).

Structural features of siRNA have been studied for decades. The classical structure of siRNAs requires an appropriate duplex length, 3' overhang, and asymmetrical structure. From a study in *Drosophila melanogaster*, the standard siRNA design was proposed to be dsRNAs of 21 nt sense/antisense strands forming a 19 base-pair (bp) dsRNA stem with 2 nt 3' overhangs at both ends (Elbashir *et al*., 2001b). However, in mammalian cells, recent studies showed that non-canonical siRNA could be as effective as classical siRNAs or could even be improved by variations in length, symmetry, and overhang. siRNAs without 3' overhang(s) (Czauderna *et al*., 2003; Rose *et al*., 2005; Chang *et al*., 2007), and those longer (Kim *et al*., 2005) or shorter (Chu and Rana, 2008) than 19 bp were also effective in gene silencing in mammalian cells. Asymmetry in 3' overhang structure, only at the antisense strand, resulted in better performance than symmetric siRNAs (Sano *et al*., 2008).

For effective and specific knockdown of mRNA targets, rational design of siRNAs is critical. First generation algorithms for siRNA design were developed based on thermodynamic stability (Schwarz *et al*., 2003), positional preference (Amarzguioui and Prydz, 2004; Reynolds *et al*., 2004; Ui-Tei *et al*., 2004), and uniqueness of the target sequence (Pancoska *et al*., 2004). These studies suggested that functional siRNAs are asymmetrical in the stability of the duplex ends as seen by the unstable 5' terminus of guide strands, and the fact that 5' termini of guide strands prefer the bases A or U. Additionally, evaluation of target site accessibility between siRNA and mRNA is critical, and is calculated based on the energy required for opening the binding site and forming hybridization (Muckstein *et al*., 2006; Tafer *et al*., 2008). To enhance prediction accuracy, second generation algorithms utilized new models with a large number of observations. They applied an artificial neural network model (Huesken *et al*., 2005) or a linear regression model (Shabalina *et al*., 2006; Vert *et al*., 2006; Ichihara *et al*., 2007).

In this study, we took various conditions into account to design efficient human tyrosinase siRNAs. To maximize efficiency in siRNA design, we combined known criteria for evaluation using multiple siRNA design algorithms (*RNAxs*, *i-Score*, and *siRNA scales*): target site accessibility, GC content, relative thermodynamic stability at both ends, as well as other criteria. We further demonstrated the inhibitory effect of selected siRNAs on melanin production in human melanoma cells.

MATERIALS AND METHODS

Combinatorial application of siRNA design algorithms and synthesis

For the mRNA sequence of human tyrosinase (*TYR*), the reference sequence (Refseq id NM_000372) from the NCBI nucleotide database was utilized. To evaluate target accessibility, the *RNAxs* design tool was used (http://rna.tbi.univie.ac.at/cgi-bin/RNAxs/). *RNAxs* combines known siRNA functionality criteria (asymmetry, self-folding, free-end) with RISC target site accessibility (Tafer *et al*., 2008). 272 siRNAs passed with default parameters (8 nt accessibility threshold; 0.01157, 16 nt accessibility threshold; 0.001002, self-folding energy; 0.9022, sequence asymmetry; 0.5, energy asymmetry; 0.4655, free end; 0.625) in all criteria and were ranked by score. *i-Score* and *siRNA scales* are based on a linear regression model and were trained using the Huesken dataset (Huesken *et al*., 2005). The *i-Score* (inhibitory–Score) algorithm calculates ΔG values of siRNA strands, dinucleotides at the 5' and 3' ends,

Table 1. Selected siRNA sequences for human tyrosinase (NM_000372)

	position	sense	Antisense	*siRNA scales*	*i-Score*	Whole ΔG
1	241	CCUUCCGUCUUUUAUAAUA	UAUUAUAAAAGACGGAAGGcc	11	75.0	-30.8
2	412	CUCACUUUAGCAAAGCAUA	UAUGCUUUGCUAAAGUGAGgu	11	71.2	-33.4
3	464	CCUAUGGCCAAAUGAAAAA	UUUUUCAUUUGGCCAUAGGuc	9	71.9	-33.0
4	471	CCAAAUGAAAAAUGGAUCA	UGAUCCAUUUUUCAUUUGGcc	20	70.1	-30.9
5	472	CAAAUGAAAAAUGGAUCAA	UUGAUCCAUUUUUCAUUUGgc	11	70.7	-28.5
6	485	GAUCAACACCCAUGUUUAA	UUAAACAUGGGUGUUGAUCca	6	75.9	-33.5
7	494	CCAUGUUUAACGACAUCAA	UUGAUGUCGUUAAACAUGGgu	0	80.5	-32.6
8	495	CAUGUUUAACGACAUCAAU	AUUGAUGUCGUUAAACAUGgg	12	70.9	-30.4
9	498	GUUUAACGACAUCAAUAUU	AAUAUUGAUGUCGUUAAACau	20	69.5	-28.4
10	500	UUAACGACAUCAAUAUUUA	UAAAUAUUGAUGUCGUUAAac	24	67.0	-27.5
11	510	CAAUAUUUAUGACCUCUUU	AAAGAGGUCAUAAAUAUUGau	12	74.7	-29.1
12	582	CUGGAGAGACAUUGAUUUU	AAAAUCAAUGUCUCUCCAGau	19	67.6	-33.5
13	679	GGAGAUGAAAACUUCACUA	UAGUGAAGUUUUCAUCUCCug	2	75.2	-33.8
14	680	GAGAUGAAAACUUCACUAU	AUAGUGAAGUUUUCAUCUCcu	15	69.7	-31.6
15	681	AGAUGAAAACUUCACUAUU	AAUAGUGAAGUUUUCAUCUcc	27	69.7	-30.1
16	852	CCAUCAGUCUUUAUGCAAU	AUUGCAUAAAGACUGAUGGcu	8	69.2	-33.6
17	856	CAGUCUUUAUGCAAUGGAA	UUCCAUUGCAUAAAGACUGau	4	79.5	-33.4
18	966	GAGUUUGACCCAAUAUGAA	UUCAUAUUGGGUCAAACUCag	3	74.7	-33.7
19	967	AGUUUGACCCAAUAUGAAU	AUUCAUAUUGGGUCAAACUca	20	65.9	-32.4
20	1016	GCUUUAGAAAUACACUGGA	UCCAGUGUAUUUCUAAAGCug	11	67.2	-33.7
21	1017	CUUUAGAAAUACACUGGAA	UUCCAGUGUAUUUCUAAAGcu	9	73.0	-31.2
22	1022	GAAAUACACUGGAAGGAUU	AAUCCUUCCAGUGUAUUUCua	7	69.4	-33.7
23	1094	CCUUGCACAUCUAUAUGAA	UUCAUAUAGAUGUGCAAGGca	7	75.1	-34.0
24	1099	CACAUCUAUAUGAAUGGAA	UUCCAUUCAUAUAGAUGUGca	16	66.3	-32.0
25	1168	CAUGCAUUUGUUGACAGUA	UACUGUCAACAAAUGCAUGgu	10	66.4	-33.3
26	1171	GCAUUUGUUGACAGUAUUU	AAAUACUGUCAACAAAUGCau	12	71.1	-30.9
27	1173	AUUUGUUGACAGUAUUUUU	AAAAAUACUGUCAACAAAUgc	26	67.6	-27.2
28	1305	UGGUGAUUUCUUUAUUUCA	UGAAAUAAAGAAAUCACCAuu	21	71.0	-30.0
29	1306	GGUGAUUUCUUUAUUUCAU	AUGAAAUAAAGAAAUCACCau	8	76.1	-29.0
30	1338	CUAUGACUAUAGCUAUCUA	UAGAUAGCUAUAGUCAUAGcc	14	74.5	-32.8
31	1372	GACUCUUUUCAAGACUACA	UGUAGUCUUGAAAAGAGUCug	10	68.8	-33.7
32	1375	UCUUUUCAAGACUACAUUA	UAAUGUAGUCUUGAAAAGAgu	15	67.4	-30.3
33	1376	CUUUUCAAGACUACAUUAA	UUAAUGUAGUCUUGAAAAGag	11	70.8	-28.8
34	1572	GUAUCAGAGCCAUUUAUAA	UUAUAAAUGGCUCUGAUACaa	11	74.7	-32.0

34 siRNA sequences were selected that passed the thresholds from target accessibility evaluation, *i-Score*, *siRNA scales*, and ΔG.

the maximum GC stretch length and GC content (http://www.med.nagoya-u.ac.jp/neurogenetics/i_Score/i_score.html/) (Ichihara *et al*., 2007). This algorithm identifies the preferred base for each nucleotide position by calculating the inhibition score (*i-Score*). Also, to improve score design accuracy, we selected less thermostable siRNAs with whole ΔG values ≥-34.6 kcal/mol (Ichihara *et al*., 2007). *siRNA scales* calculates the stability of 5' and 3' ends and total GC content (http://gesteland.genetics.utah.edu/siRNA_scales/index.html/) (Matveeva *et al*., 2007). We applied filters of the scores to be *i-Score* ≥65 and *siRNA scales* ≤30. All siRNAs for TYR were synthesized by Bioneer Inc. (Dajeon, Korea) as 21-mers with a 3' overhang on the antisense strand. See Table 1 for the full list of siRNAs.

Cell culture

The highly pigmented human melanoma cell line MNT-1 was kindly provided by Dr. Minsoo Noh (Seoul National University, School of Pharmacy). Cells were maintained in Minimal Essential Medium (MEM) supplemented with 20% fetal bovine serum (FBS), 10% Dulbecco's Modified Eagle Medium (DMEM), and gentamicin (50 μg/mL). Trypsin (0.25%) and ethylenediaminetetraacetic acid (EDTA) were purchased from Gigbco-BRL, and 20 mM HEPES was purchased from Sigma (St. Louis, MO, USA). Cells were maintained at 37°C in a humidified atmosphere of 5% CO_2 in air.

siRNA transfection

Lipofectamine 2000 (11668-027, Invitrogen, Waltham, MA, USA) or DharmaFECT (T-2001-02, Thermo Scientific, Walltham, MA, USA) was used for cell transfection according to the manufacturer's protocol. 34 anti-Tyrosinase siRNAs and non-targeting siRNA were purchased from Bioneer Inc. Positive control siRNA was purchased from Santa Cruz (#sc-36766, Santa Cruz, Dallas, TX, USA). MNT-1 cells were grown to 60% confluence and transfected with either Lipofectamine or DharmaFECT reagent depending on the protocol of manufacturer.

Immunoblot analysis

MNT-1 cells were lysed with lysis buffer (20 mM tris pH 7.5,

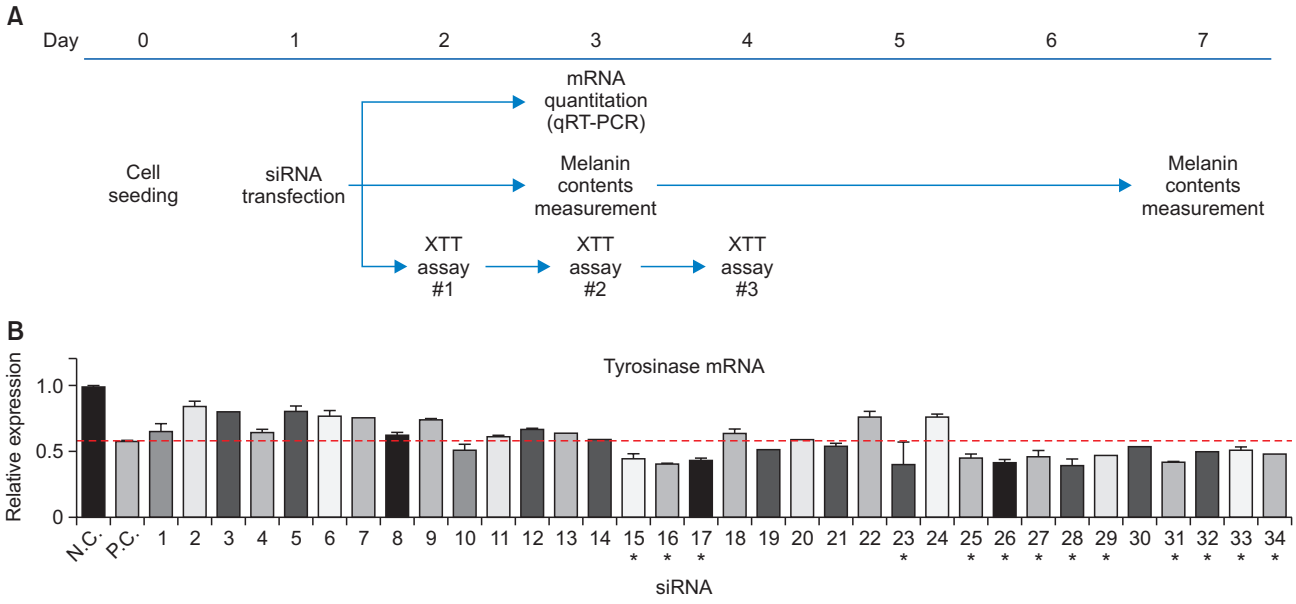

Fig. 2. Screening for optimal tyrosinase siRNA sequences. (A) Experimental scheme of the study. (B) MNT-1 cells were transfected with siRNAs for negative control (N.C.), positive control (P.C. #1) or tyrosinase (#1 to #34). The relative expression level of tyrosinase 2 days after transfection is presented as a bar graph. *Indicates the 13 siRNAs showing higher knockdown efficiency than the positive control (P.C. #1). Significant difference was determined by one way ANOVA. Data are shown as means ± SD.

5 mM EDTA, 10 mM $Na_4P_2O_7$, 100 mM NaF, 2 mM Na_3VO_4, 1% NP-40, 1 mM PMSF, 10 μg/mL aprotinin, and 10 μg/mL leupeptin) and 15 μg of protein was subjected to SDS-PAGE, and transferred to nitrocellulose membrane. The membranes were incubated with an anti-tyrosinase antibody (#sc-7834, Santa Cruz). The bands were visualized with a ChemiDoc imaging system (Bio-Rad, Hercules, CA, USA) and quantified by ImageJ software (ver. 1.44p, NIH, USA).

Measurement of melanin content

Melanin content was measured as described previously (Hosoi *et al*., 1985) with some modifications. Briefly, MNT-1 cells were seeded onto 6-well plates (6×10^5 cells/well) and transfected with siRNA. At 48 h and 168 h after transfection, cells were washed with phosphate-buffered saline (PBS) and harvested. After washing with PBS, cell pellets were dissolved in 1 mL of 1 N NaOH containing 10% DMSO and incubated for 1 h at 80°C. The absorbance of the solution was measured at 450 nm. Melanin content was calculated based on a standard curve obtained from synthetic melanin.

Cell viability test (XTT assay)

The XTT assay (cat# 11465015001, Roche, Pleasanton, CA, USA) was performed according to the Manufacturer's protocol. Briefly, 6×10^5 MNT1 cells/well were plated in 6-well plates. On the next day, cells were transfected with individual siRNAs. After 24 h, cells were plated in 96-well microplates in quintuplicate, and then were additionally maintained for the indicated number of days. For XTT assay, 50 μL of XTT labeling mixture (XTT-labeling reagent:electron-coupling reagent=50:1 to reach a final XTT concentration of 0.3 mg/mL) was added to each well and the plates were incubated at 37°C in a 5% CO_2 atmosphere for 4 h. Absorbance was measured with an enzyme-linked immunosorbent assay plate reader at 450 nm.

RNA isolation and quantitative real-time polymerase chain reaction (PCR) analysis

Total RNA was extracted from cells using an easy-BLUE kit (the TRIzol reagent, iNtRON, Seongnam, Korea), according to the manufacturer's protocol. TRIzol was removed by the addition of chloroform and mRNA was precipitated with isopropanol. RNA precipitates were washed with 75% ethanol. Optical densities at 260 and 280 nm were measured using a UV spectrometer to assess RNA quantity and purity, and RNA integrity was confirmed by agarose gel electrophoresis. Gene-specific primers were designed to amplify human tyrosinase (TYR), Tumor necrosis factor α (TNF), interleukin 6 (IL6) and the housekeeping gene glyceraldehyde 3-phosphate dehydrogenase (GAPDH) for an internal control. The following primer pairs were used for TYR (F: 5′-GCCAACGATCCTAT CTTCCTTC-3′, R: 5′-GTGCATTG-GCTTCTGGATAAAC-3′), TNF (F: 5′-GAGGCCAAGCCCTG-GTATG-3′, R: 5′-CGGGCCGATTGATCTCAGC-3′), IL6 (F: 5′-CTGGATTCAATGAGGAGACTTG-3′ R: 5′-CACTACTCT-CAAATCTGTTCTGG-3′) and GAPDH (F: 5′-GTGATGGCATG-GACTGTGGT-3′, R: 5′-AAGGGTCATCATCTCTGCCC-3′). All amplifications were conducted using a pre-mixture (20 μL) containing 500 nmol/L of gene-specific primers and 2 μL of template RNA under the following conditions: denaturation at 95°C for 1 min, followed by 45 cycles of 95°C for 20 s, 58°C for 20 s, and 72°C for 25 s, with a final extension at 72°C for 5 min.

Statistical analysis

Graphical data are presented as mean ± SD. Statistical significance among triplicates and between groups were determined using one- or two-way analysis of variance (ANOVA) followed by a Bonferroni multiple comparisons post-test or Student's *t*-test, respectively. Significance was assumed when $p<0.05$.

RESULTS

Design of human tyrosinase siRNAs

To build an efficient siRNA pool targeting human tyrosinase, we applied bioinformatics tools combining several advanced prediction models. We obtained the mRNA reference sequence (Refseq id NM_000372) from NCBI nucleotide dataset for human tyrosinase and excluded 5'UTR and 3'UTR regions from the prediction, because they can interfere with RISC function (Elbashir *et al*., 2002). First, the sequence was evaluated for RISC accessibility to the target site using *RNAxs* software, which is considered an important factor for restricting RISC's endonucleolytic activity (Tafer *et al*., 2008). Beside target accessibility, this algorithm also evaluates self-folding energy and sequence asymmetry to calculate scores. From this algorithm, 272 19-mer double stranded sequences (17% of 1,572 sequences) passed the default threshold. Sequences were also evaluated by two second generation algorithms based on linear regression models: *i-Score* (inhibitory–Score) (Ichihara *et al*., 2007) and *siRNA scales* (Matveeva *et al*., 2007). Both *i-Score* and *siRNA scales* algorithms consider nucleotide position-dependent preference. *siRNA scales* calculates local duplex stability and total G/C content for evaluation of functional siRNAs. We applied filters for *i-Score* ≥65 and for *siRNA scales* ≤30, with whole ΔG≥-34.6 kcal/mol. We found that *i-Score* was more strict, passing 191 sequences (12%), whereas *siRNA scales* was less strict, passing 47% of sequences. Finally, 71 siRNAs were obtained that met the criteria of all three siRNA design algorithms. When whole ΔG value limitations were applied, only 34 siRNAs (2.2%) finally passed without off-target effects, as determined by using the NCBI nucleotide database (Fig. 1A, 1B). For this study, we designed 19-bp RNA duplexes with an asymmetric 2-nt overhang at the 3' end of the antisense strand for better performance as suggested (Fig. 1C) (Rose *et al*., 2005; Sano *et al*., 2008). The full siRNA sequences are listed in Table 1.

Evaluation of tyrosinase siRNA efficacy in the human melanoma cell line MNT-1

To evaluate the efficacy of siRNAs selected by siRNA design tools, we transfected MNT-1 cells with 34 individual siRNAs and measured tyrosinase mRNA (*TYR*) expression by qRT-PCR. As shown in the experimental scheme described in Fig. 2A, tyrosinase mRNA expression levels were measured on day 2 after transfection. The 34 siRNAs reduced tyrosinase mRNA levels by an average of 57.8% (SD=0.141) in the first screening. 13 siRNAs were more effective than the commercially available siRNA, which was used as positive control (P.C.) with significance (Fig. 2B, Table 2). We further quantified tyrosinase mRNA to confirm the efficacy of the 6 most effective (#16, 17, 23, 26, 28, and 31) and 3 least effective (#2, 3, and 5) siRNAs. In accordance with the first screening, the 6 most effective siRNAs knocked down tyrosinase expression efficiently (0.294-fold vs. N.C.) and also were more effective than the positive control (0.39-fold vs. N.C.), whereas the 3 least effective siRNAs showed similar or lower efficacy (Fig. 3A, 3B). In the second screening, even the least effective siRNAs knocked down tyrosinase expression approximately 0.5-fold. To see if siRNAs decrease tyrosinase protein level, we performed immunoblot analysis. In accordance with the result from mRNA levels, tyrosinase protein level was decreased effectively (Fig. 3C). Generally, the 6 most effective siRNAs showed better performance than the 3 least effective ones. Considering the effective knockdown provided by even our worst-performing siRNAs, our results support the idea that siRNA production by combining multiple siRNA design algorithms was an efficient approach.

Table 2. Relative expression level of tyrosinase mRNA after siRNA transfection

siRNA #	Test 1	Test 2	Mean	Order of efficiency	Second test
N.C.	1.00	0.98	0.99		
P.C.	0.58	0.56	0.57		
1	0.70	0.59	0.65	25	
2	0.87	0.81	0.84	34	*
3	0.80	0.80	0.80	32	*
4	0.62	0.66	0.64	24	
5	0.77	0.84	0.80	33	*
6	0.80	0.73	0.77	31	
7	0.76	0.76	0.76	29	
8	0.64	0.61	0.62	21	
9	0.75	0.73	0.74	27	
10	0.54	0.46	0.50	13	
11	0.62	0.60	0.61	20	
12	0.67	0.66	0.67	26	
13	0.63	0.64	0.63	22	
14	0.59	0.58	0.59	18	
15	0.42	0.47	0.45	8	
16	0.40	0.41	0.40	2	*
17	0.41	0.44	0.43	6	*
18	0.61	0.66	0.63	23	
19	0.51	0.51	0.51	15	
20	0.59	0.58	0.59	19	
21	0.52	0.55	0.54	17	
22	0.79	0.73	0.76	30	
23	0.52	0.28	0.40	3	*
24	0.73	0.77	0.75	28	
25	0.47	0.42	0.44	7	
26	0.43	0.38	0.41	4	*
27	0.49	0.42	0.45	9	
28	0.42	0.35	0.39	1	*
29	0.47	0.46	0.47	10	
30	0.53	0.53	0.53	16	
31	0.42	0.40	0.41	5	*
32	0.50	0.49	0.50	12	
33	0.49	0.53	0.51	14	
34	0.48	0.48	0.48	11	

Average relative expression level compared to the negative control siRNA (N.C.) were presented.

Anti-melanogenic effect of siRNAs in MNT-1 cells

The above results indicate that the siRNAs we designed could downregulate melanin synthesis in melanin-producing cells. To test the effect of our siRNAs (#16, 17, 26) on melanin synthesis by tyrosinase, we measured melanin content in siRNA-transfected MNT-1 cells. As shown in Fig. 4A (upper), melanin content was only minimally changed on day 2 after transfection. However, when melanin content was analyzed on day 7, the anti-melanogenic effect of these siRNAs was

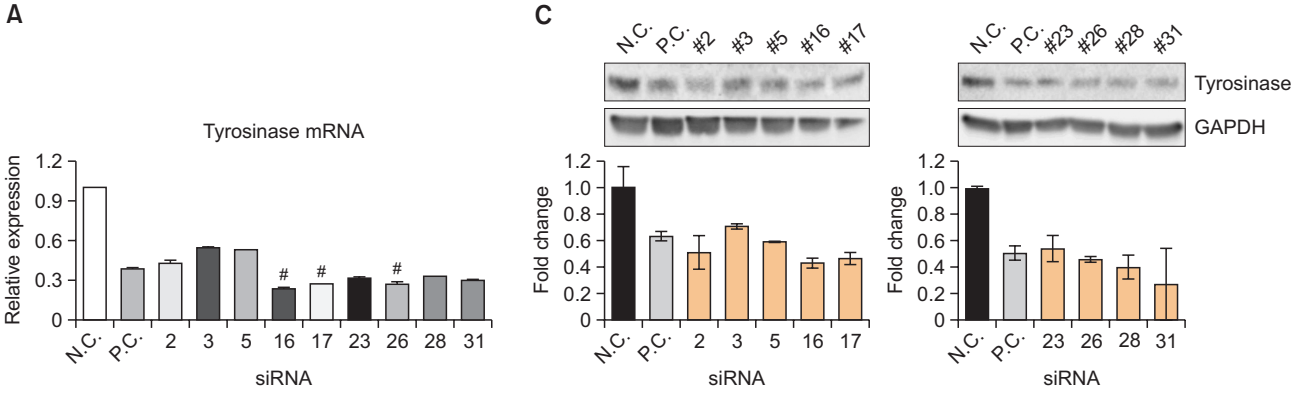

B

siRNA #	Test 1	Test 2	Mean	Significance (vs. P.C.)
N.C.	1.00	1.00	1.00	
P.C.	0.38	0.39	0.39	
2	0.41	0.44	0.43	
3	0.54	0.55	0.55	
5	0.53	0.53	0.53	
16	0.23	0.24	0.24	***
17	0.27	0.27	0.27	***
23	0.31	0.32	0.32	**
26	0.28	0.29	0.29	***
28	0.33	0.33	0.33	***
31	0.29	0.30	0.30	***

Fig. 3. Effective anti-melanogenesis by tyrosinase siRNA sequence. MNT-1 cells were transfected with siRNA for negative control (N.C.), positive control (P.C.), or tyrosinase (top 6 siRNAs and bottom 3 siRNAs among the 34 siRNA candidates) for a second screening. (A) The relative expression level of tyrosinase at day 2 after transfection is presented as a bar graph. Data are means ± SD. # indicates the top 3 siRNAs with highest knockdown efficiency. Significant difference was determined by one way ANOVA. (B) Average expression levels compared to the negative control siRNA (N.C.) are presented. **p<0.01; ***p<0.001 versus positive control. (C) Tyrosinase protein level was measured by immunoblot analysis using anti-tyrosinase antibody. GAPDH was used as a loading control.

detected (Fig. 4A, lower). Colorimetric measurement of these samples (day 7) indicated that all siRNAs significantly reduced melanin content (p<0.001). siRNAs #16 and 17 were as effective as the positive control in reducing melanin content by approximately 0.55-fold (0.56-fold by P.C.) although siRNA #26 was less effective (~0.74-fold) (Fig. 4B). These data show that the siRNAs we designed are effective in reducing melanin synthesis in cells.

The effect of siRNAs on cell viability

Some siRNAs result in toxicity, affecting cell viability by off-target effects related to cell growth, death, and other properties. To identify if these siRNAs result in cell toxicity, we analyzed cell viability by observing changes in cell morphology and by XTT assays in siRNA-transfected MNT-1 cells. On day 1 or 2 after siRNA transfection (#16, 17, 26, and P.C.), no significant change in cell morphology was observed (Fig. 5A). Additionally, no discernible change in cell viability was seen as measured by XTT assay (Fig. 5B). We further tested if these siRNAs can induce immune response by measuring mRNA levels of TNFα and IL-6. siRNA #16 and 17 had no effect on TNFα mRNA expression while #26 showed increase around 1.8-fold in both naked and liposome aided conditions (Fig. 5C). However, the level was not higher than that of positive control (P.C.). In contrast, IL-6 was upregulated by all three siRNAs in liposome aided condition while the positive control showed no harmful effect. Especially, siRNA #26 and P.C. triggered immune responses even in naked state, in which no reduction of tyrosinase mRNA was detected. Altogether, our data showed that combining siRNA design algorithms is an efficient approach for developing novel siRNA sequences. In addition, the selected siRNAs (#16 and 17) were effective in suppressing synthesis of human melanin, suggesting that these siRNAs could be further developed as novel siRNA sequences for use in biomedical research and cosmetic fields.

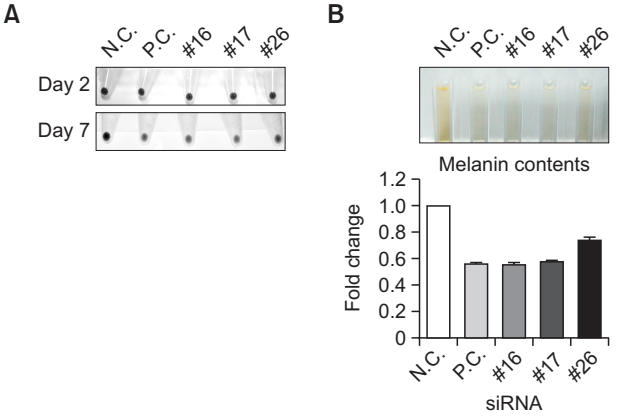

Fig. 4. Anti-melanogenic effect of the top 3 siRNAs. (A) Images of the cell pellet at day 2 (upper) and 7 (lower) after siRNA transfection. (B) The melanin content from the cell pellet of at day 7 after siRNA transfection is shown as a bar graph. Images of melanin level after each siRNA transfection are shown (upper). Data are shown as means ± SD.

DISCUSSION

Skin-lightening agents are useful for cosmetic purposes and many such formulations have been developed for decades. Currently, various agents are available, with diverse mechanisms of action such as tyrosinase inhibition (hydroquinone, azelaic acid, arbutin), stimulation of keratinocyte turnover and reduction of melanosome transfer (retinoids), cop-

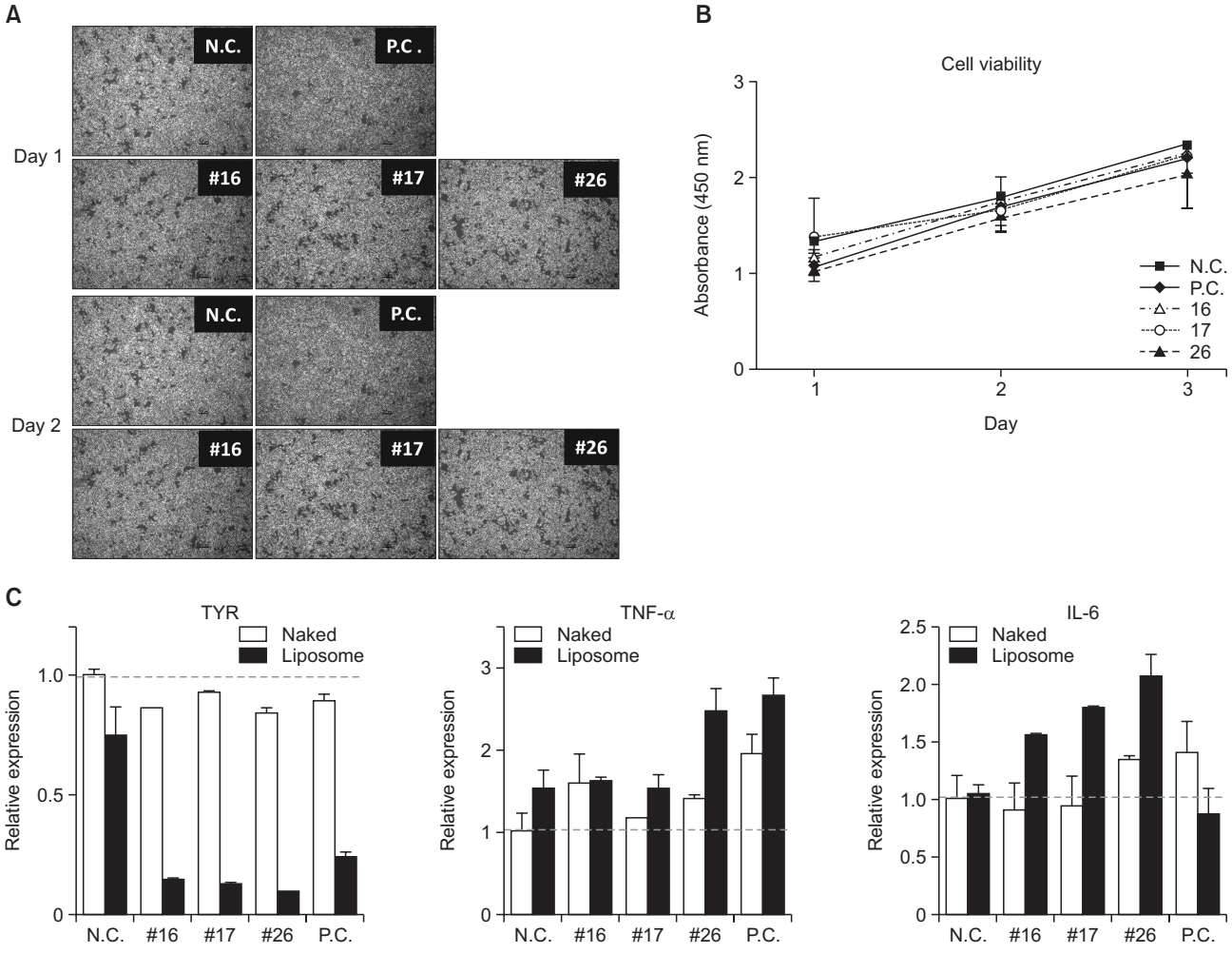

Fig. 5. Negligible effects of siRNA transfection on proliferation. (A) microscopic images of MNT-1 cells at day 1 (upper panels) and day 2 (lower panels) after the indicated siRNA transfection. (B) Cell viability after transfection with the indicated siRNA was determined at days 1, 2, and 3. Data are shown as means ± SD. (C) mRNA expression of Tyrosinase, TNFa and IL6 after siRNA transfection with or without transfection reagent was measured with real-time PCR (N.C.: negative control, and P.C.: positive control). Data are shown as means ± SD.

per chelation (kojic acid and ascorbic acid), and inhibition of melanosome maturation (arbutin) (Sheth and Pandya, 2011). Tyrosinase is a rate-limiting enzyme in melanin production from melanocytes (Lerner and Fitzpatrick, 1950; Hearing and Tsukamoto, 1991). Here, we sought to reduce tyrosinase expression by applying tyrosinase siRNAs designed using multiple prediction tools.

Efficient siRNA design is crucial, as even subtle sequence changes may significantly alter functionality. Currently, numerous siRNA design algorithms have been developed and these algorithms consider diverse factors to be critical for functionality, such as target accessibility, secondary mRNA structures, and positional preferences of siRNA sequence. Early studies on rules for preferred siRNA sequence patterns were suggested: N2SN17WN2 by Ui-Tei rule (Ui-Tei *et al*., 2004), N4AN6TN2HN5WN2 by Reynolds (Reynolds *et al*., 2004) and so on. These rules also commonly indicate that an asymmetrical siRNA structure is critical: more A/U bases are necessary at the 5'-end of the antisense strand whereas more G/C bases are necessary at the 5'-end of the sense strand. Low GC content in the 5'-end of the antisense strand is considered to aid in unwinding and incorporation of the siRNA duplex into the RISC complex.

i-Score and *siRNA scales* algorithms calculate nucleotide preference at each position of siRNA in addition to other factors. For that reason, scores from *i-Score* and *siRNA scales* algorithms showed a mild to moderate correlation (R^2=0.4309) (data not shown) and most siRNAs that passed the requirements of the *i-Score* algorithm were included in *siRNA scales*. Our results also showed that the default threshold provided by *siRNA scales* is less strict than *i-Score* (47% vs. 12% from total).

Previous studies suggested that the siRNA secondary structure whole ΔG values are a critical determinant in siRNA efficiency (Ichihara *et al*., 2007; Ladunga, 2007). Especially, siRNAs with ΔG values less than -34.6 kcal/mol, which are thermodynamically stable, showed poor knockdown efficiency (Ichihara *et al*., 2007). When we calculated the correlation coefficient between ΔG values and suppression levels using our data, no significant correlation was observed (data not shown). However, since we only examined a small number of siRNAs, we cannot conclude that ΔG values are statisti-

cally unrelated to siRNA efficiency. To clearly determine the effect of whole ΔG values on siRNA activity, a large number of samples is needed and siRNAs with lower whole ΔG values should be added in the test for comparison.

Collectively, we designed human tyrosinase siRNAs using multiple algorithms and parameters and identified highly efficient siRNAs that may be useful in the cosmetic field. In fact, many siRNAs are currently being considered for use in biomedicine and cosmetic fields, and have been tested in clinical trials worldwide. However, for the broad usage of siRNA-based applications, some barriers remain to be resolved such as issues with safety, stability, and delivery.

ACKNOWLEDGMENTS

This study was supported by a grant from Leaders Cosmetics, Sansung L&S Co., Ltd (#2015/05/20-31) and by Basic Science Research Program through the National Research Foundation of Korea (KRF) funded by the Ministry of Education (2016R1D1A1B01012515).

REFERENCES

Amarzguioui, M. and Prydz, H. (2004) An algorithm for selection of functional siRNA sequences. *Biochem. Biophys. Res. Commun.* **316**, 1050-1058.

Chang, C. I., Hong, S. W., Kim, S. and Lee, D. K. (2007) A structure-activity relationship study of siRNAs with structural variations. *Biochem. Biophys. Res. Commun.* **359**, 997-1003.

Chu, C. Y. and Rana, T. M. (2008) Potent RNAi by short RNA triggers. *RNA* **14**, 1714-1719.

Czauderna, F., Fechtner, M., Dames, S., Aygun, H., Klippel, A., Pronk, G. J., Giese, K. and Kaufmann, J. (2003) Structural variations and stabilising modifications of synthetic siRNAs in mammalian cells. *Nucleic Acids Res.* **31**, 2705-2716.

Elbashir, S. M., Harborth, J., Lendeckel, W., Yalcin, A., Weber, K. and Tuschl, T. (2001a) Duplexes of 21-nucleotide RNAs mediate RNA interference in cultured mammalian cells. *Nature* **411**, 494-498.

Elbashir, S. M., Harborth, J., Weber, K. and Tuschl, T. (2002) Analysis of gene function in somatic mammalian cells using small interfering RNAs. *Methods* **26**, 199-213.

Elbashir, S. M., Martinez, J., Patkaniowska, A., Lendeckel, W. and Tuschl, T. (2001b) Functional anatomy of siRNAs for mediating efficient RNAi in Drosophila melanogaster embryo lysate. *EMBO J.* **20**, 6877-6888.

Engels, J. W. (2013) Gene silencing by chemically modified siRNAs. *N. Biotechnol.* **30**, 302-307.

Fire, A., Xu, S., Montgomery, M. K., Kostas, S. A., Driver, S. E. and Mello, C. C. (1998) Potent and specific genetic interference by double-stranded RNA in Caenorhabditis elegans. *Nature* **391**, 806-811.

Gillbro, J. M. and Olsson, M. J. (2011) The melanogenesis and mechanisms of skin-lightening agents--existing and new approaches. *Int. J. Cosmet. Sci.* **33**, 210-221.

Hearing, V. J. and Tsukamoto, K. (1991) Enzymatic control of pigmentation in mammals. *FASEB J.* **5**, 2902-2909.

Hosoi, J., Abe, E., Suda, T. and Kuroki, T. (1985) Regulation of melanin synthesis of B16 mouse melanoma cells by 1 alpha, 25-dihydroxyvitamin D3 and retinoic acid. *Cancer Res.* **45**, 1474-1478.

Huesken, D., Lange, J., Mickanin, C., Weiler, J., Asselbergs, F., Warner, J., Meloon, B., Engel, S., Rosenberg, A., Cohen, D., Labow, M., Reinhardt, M., Natt, F. and Hall, J. (2005) Design of a genome-wide siRNA library using an artificial neural network. *Nat. Biotechnol.* **23**, 995-1001.

Ichihara, M., Murakumo, Y., Masuda, A., Matsuura, T., Asai, N., Jijiwa, M., Ishida, M., Shinmi, J., Yatsuya, H., Qiao, S., Takahashi, M. and Ohno, K. (2007) Thermodynamic instability of siRNA duplex is a prerequisite for dependable prediction of siRNA activities. *Nucleic Acids Res.* **35**, e123.

Kim, D. H., Behlke, M. A., Rose, S. D., Chang, M. S., Choi, S. and Rossi, J. J. (2005) Synthetic dsRNA Dicer substrates enhance RNAi potency and efficacy. *Nat. Biotechnol.* **23**, 222-226.

Ladunga, I. (2007) More complete gene silencing by fewer siRNAs: transparent optimized design and biophysical signature. *Nucleic Acids Res.* **35**, 433-440.

Lerner, A. B. and Fitzpatrick, T. B. (1950) Biochemistry of melanin formation. *Physiol. Rev.* **30**, 91-126.

Matveeva, O., Nechipurenko, Y., Rossi, L., Moore, B., Saetrom, P., Ogurtsov, A. Y., Atkins, J. F. and Shabalina, S. A. (2007) Comparison of approaches for rational siRNA design leading to a new efficient and transparent method. *Nucleic Acids Res.* **35**, e63.

Muckstein, U., Tafer, H., Hackermuller, J., Bernhart, S. H., Stadler, P. F. and Hofacker, I. L. (2006) Thermodynamics of RNA-RNA binding. *Bioinformatics* **22**, 1177-1182.

Pancoska, P., Moravek, Z. and Moll, U. M. (2004) Efficient RNA interference depends on global context of the target sequence: quantitative analysis of silencing efficiency using Eulerian graph representation of siRNA. *Nucleic Acids Res.* **32**, 1469-1479.

Reynolds, A., Leake, D., Boese, Q., Scaringe, S., Marshall, W. S. and Khvorova, A. (2004) Rational siRNA design for RNA interference. *Nat. Biotechnol.* **22**, 326-330.

Rose, S. D., Kim, D. H., Amarzguioui, M., Heidel, J. D., Collingwood, M. A., Davis, M. E., Rossi, J. J. and Behlke, M. A. (2005) Functional polarity is introduced by Dicer processing of short substrate RNAs. *Nucleic Acids Res.* **33**, 4140-4156.

Sano, M., Sierant, M., Miyagishi, M., Nakanishi, M., Takagi, Y. and Sutou, S. (2008) Effect of asymmetric terminal structures of short RNA duplexes on the RNA interference activity and strand selection. *Nucleic Acids Res.* **36**, 5812-5821.

Schwarz, D. S., Hutvagner, G., Du, T., Xu, Z., Aronin, N. and Zamore, P. D. (2003) Asymmetry in the assembly of the RNAi enzyme complex. *Cell* **115**, 199-208.

Shabalina, S. A., Spiridonov, A. N. and Ogurtsov, A. Y. (2006) Computational models with thermodynamic and composition features improve siRNA design. *BMC Bioinformatics* **7**, 65.

Sheth, V. M. and Pandya, A. G. (2011) Melasma: a comprehensive update: part II. *J. Am. Acad. Dermatol.* **65**, 699-714.

Slominski, A., Tobin, D. J., Shibahara, S. and Wortsman, J. (2004) Melanin pigmentation in mammalian skin and its hormonal regulation. *Physiol. Rev.* **84**, 1155-1228.

Tafer, H., Ameres, S. L., Obernosterer, G., Gebeshuber, C. A., Schroeder, R., Martinez, J. and Hofacker, I. L. (2008) The impact of target site accessibility on the design of effective siRNAs. *Nat. Biotechnol.* **26**, 578-583.

Ui-Tei, K., Naito, Y., Takahashi, F., Haraguchi, T., Ohki-Hamazaki, H., Juni, A., Ueda, R. and Saigo, K. (2004) Guidelines for the selection of highly effective siRNA sequences for mammalian and chick RNA interference. *Nucleic Acids Res.* **32**, 936-948.

Vert, J. P., Foveau, N., Lajaunie, C. and Vandenbrouck, Y. (2006) An accurate and interpretable model for siRNA efficacy prediction. *BMC Bioinformatics* **7**, 520.